HNPS Advances in Nuclear Physics

Vol 15 (2006)

HNPS2006

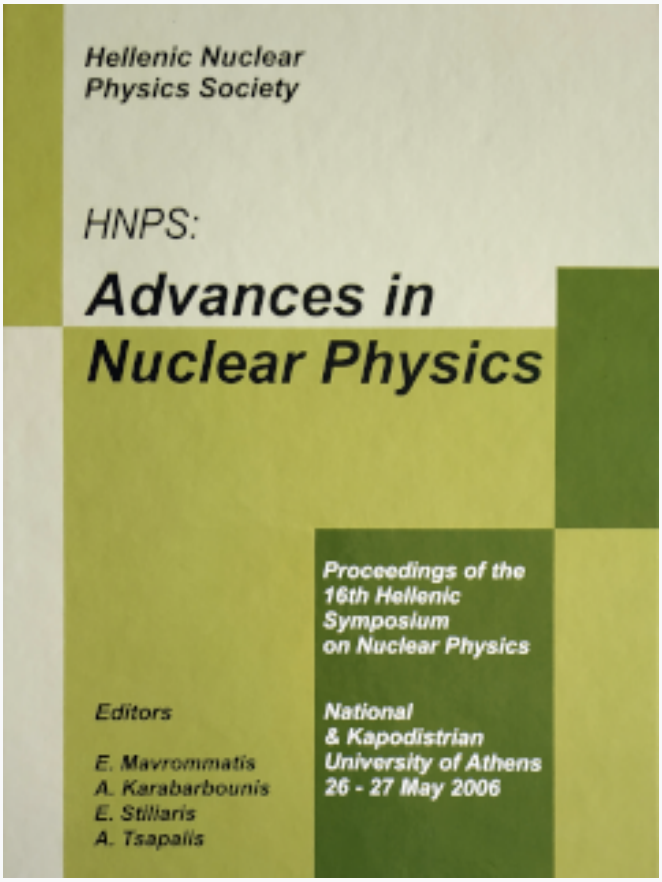

Nucleon Electromagnetic Structure from Lattice QCD

C. Alexandrou, G. Koutsou, H. Neff, J. W. Negele, W. Schroers, A. Tsapalis

doi: 10.12681/hnps.2617

Nucleon Electromagnetic Structure from Lattice QCD

C. Alexandrou[a], G. Koutsou[a], H. Neff[b], J. W. Negele[c], W. Schroers[d] and A. Tsapalis[e] *

[a]Department of Physics, University of Cyprus, CY-1678 Nicosia, Cyprus

[b]Centre for Computational Science, Chemistry Department, University College of London, 20 Gordon Street, WC1H 0AJ, London, UK

[c]Center for Theoretical Physics, Laboratory for Nuclear Science and Department of Physics, Massachusetts Institute of Technology, Cambridge MA 02139, USA

[d]NIC/DESY Zeuthen, Platanenallee 6, D-15738 Zeuthen, Germany

[e]University of Athens, Institute for Accelerating Systems and Applications, Athens, Greece

We present an evaluation of nucleon to Δ electromagnetic form factors within Lattice QCD. The EMR and CMR ratios are calculated both in the quenched theory and using two degenerate flavors of dynamical Wilson fermions. We obtain values in qualitative agreement to experiment. In addition, we evaluate the isovector Sachs electromagnetic form factors of the nucleon both in the quenched and unquenched theory for momentum transfer squared in the range between 0.1 and 2 GeV^2. The nucleon magnetic moment and r.m.s. radii are obtained using chiral effective theory to extrapolate to the physical pion mass.

1. INTRODUCTION

Despite the apparent simplicity of the Lagrangian of Quantum Chromodynamics (QCD) it is believed to describe a wide spectrum of phenomena in the hadronic world. The low energy nonperturbative regime remains, however, out of reach to analytical methods and lattice QCD is the only applicable method. Lattice QCD is a discretized version of the continuum theory defined on finite lattice and evaluation of observable is carried out numerically within the field-theoretic path integral formulation in Euclidean time. The dependence of the observables on the lattice spacing and finite volume vanishes in a controlled manner as the lattice spacing is made smaller and the volume large enough. Besides evaluation of masses, many other hadron properties are amenable to lattice calculations, such as magnetic moments, radii, form factors and structure functions, along with strong matrix elements relevant to for weak processes, providing valuable checks of the Standard Model. A long standing problem connected to doubling of fermion species on the lattice lead to several proposals one of which was proposed by Wilson in 1974 [1]. The so called

* pea er a. . e . mp si m

Wilson fermions break chiral symmetry which is only recovered in the continuum limit. Recently the conceptual problems of having chiral fermions on the lattice were solved through a 5-dimensional formulation which leads to what it is known as Domain Wall fermions (DWF) [2]. An equivalent formulation is the construction of a Dirac operator that satisfies the Ginspang-Wilson relation known as overlap formulation [3]. In this work we will be using both Wilson fermions and DWF.

The evaluation of Euclidean path integrals on a lattice consists of two major numerical endeavors: first, the generation of a representative set of QCD configurations at sufficiently small lattice resolution and sufficiently large volume and second, the computation of the quark propagator for each member of the ensemble. The evaluation of the quark propagator requires the inversion of the lattice Dirac operator which is a huge sparse matrix of dimension $12V \times 12V$, where V is the 4-dimensional lattice volume in the case of Wilson fermions or the 5-dimensional volume for DWF. This makes the calculation of domain wall propagators an order of magnitude larger. Five years ago, due to limited computer resources, it was common practice to omit pair creation. This is known as the quenched approximation. However, during the last five years, improvements in algorithms combined with bigger computers have enable the simulation of configurations allowing pair creation of light quarks. These dynamical configurations either done with Wilson fermions or using a different fermion discretization scheme known as staggered fermions. We will use such dynamical quark configurations to study the electromagnetic properties of the nucleon and the Δ. Despite the recent progress in computer technology evaluation dynamical simulations are only possible for quark masses larger than physical. The dependence of many physical observables on the pion mass has been worked out using chiral effective theories enabling extrapolation of lattice results to the physical point.

In this talk we summarize our results on the calculation of the nucleon to Δ electromagnetic transition form factors [4] and the nucleon isovector form factors [5]. We use Wilson fermions in the quenched theory as well as with two degenerate flavors of dynamical Wilson fermions. In addition we use configurations generated using three dynamical staggered quarks. Since staggered fermions are difficult to use for the observables we want to study we used domain wall fermions for the valence quarks. Given that we obtain results using two different formulations for the dynamical quarks with different dependence on the lattice parameters agreement of the results provides a non-trivial check of consistency of our lattice methodology.

2. NUCLEON DEFORMATION AND THE $\gamma^* N \to \Delta$ FORM FACTORS

The existence of deformation in the nucleon, the fundamental constituent of matter, it is thought to be connected with quadrupole strength in the electromagnetic excitation to the $\Delta(1232)$ resonance. Precise experiments with real and virtual photons [6–9], have measured a non-zero quadrupole strength that can be accounted for if one uses deformed N and Δ states within a variety of models.

The matrix element for the N to Δ electromagnetic transition for on-shell nucleon and Δ states and real or virtual photons has the form [10]

$$\langle\, \Delta(p',s')\, |j_\mu|\, N(p,s)\rangle \;=\; i\sqrt{\frac{2}{3}}\Big(\frac{m_\Delta\, m_N}{E_\Delta(\mathbf{p}')\, E_N(\mathbf{p})}\Big)^{1/2} \bar{u}_\tau(p',s')\mathcal{O}^{\tau\mu}u(p,s) \qquad (1)$$

where p, s and p', s' denote initial and final momenta and spins and $u_\tau(p', s')$ is a spin-vector in the Rarita-Schwinger formalism. The operator $\mathcal{O}^{\tau\mu}$ can be decomposed in terms of the Sachs form factors as

$$\mathcal{O}^{\tau\mu} = \mathcal{G}_{M1}(q^2)\ K^{\tau\mu}_{M1} + \mathcal{G}_{E2}(q^2)\ K^{\tau\mu}_{E2} + \mathcal{G}_{C2}(q^2)\ K^{\tau\mu}_{C2}\ , \tag{2}$$

where the magnetic dipole, $\mathcal{G}_{M1}$, the electric quadrupole, $\mathcal{G}_{E2}$, and the Coulomb quadrupole, $\mathcal{G}_{C2}$, form factors depend on the momentum transfer squared, $q^2 = (p' - p)^2$. The exact expressions for the kinematical functions $K^{\tau\mu}$ can be found in ref. [11]. The ratios R_{EM} (or EMR) and R_{SM} (or CMR) in the rest frame of the Δ are defined via

$$R_{EM} = -\frac{\mathcal{G}_{E2}(q^2)}{\mathcal{G}_{M1}(q^2)} \quad , \quad R_{SM} = -\frac{|\mathbf{q}|}{2m_\Delta}\,\frac{\mathcal{G}_{C2}(q^2)}{\mathcal{G}_{M1}(q^2)} \quad . \tag{3}$$

The extraction of the Sachs form factors requires the computation of the three-point function

$$\begin{aligned} &\langle G^{\Delta j^\mu N}_\sigma(t_2, t_1; \mathbf{p}\,', \mathbf{p}; \Gamma)\rangle = \\ &\sum_{\mathbf{x}_2,\,\mathbf{x}_1} \exp(-i\mathbf{p}\,'\cdot\mathbf{x}_2)\exp(+i(\mathbf{p}\,'-\mathbf{p})\cdot\mathbf{x}_1)\ \Gamma^{\beta\alpha}\langle\ \Omega\mid T\left[\chi^\alpha_\sigma(\mathbf{x}_2,t_2) j^\mu(\mathbf{x}_1,t_1)\bar\chi^\beta(\mathbf{0},0)\right]\mid\Omega\ \rangle\ , \end{aligned} \tag{4}$$

along with the nucleon and Δ two-point functions

$$\begin{aligned} \langle G^{NN}(t,\mathbf{p};\Gamma)\rangle &= \sum_{\mathbf{x}} e^{-i\mathbf{p}\cdot\mathbf{x}}\ \Gamma^{\beta\alpha}\ \langle\Omega|\ T\ \chi^\alpha(\mathbf{x},t)\bar\chi^\beta(\mathbf{0},0)\ |\Omega\ \rangle \\ \langle G^{\Delta\Delta}_{\sigma\tau}(t,\mathbf{p}\,';\Gamma)\rangle &= \sum_{\mathbf{x}} e^{-i\mathbf{p}\,'\cdot\mathbf{x}}\ \Gamma^{\beta\alpha}\ \langle\Omega|\ T\ \chi^\alpha_\sigma(\mathbf{x},t)\bar\chi^\beta_\tau(\mathbf{0},0)\ |\Omega\ \rangle \quad . \end{aligned} \tag{5}$$

The nucleon source is taken at time zero, the photon is absorbed by a quark at a later time t_1 and the Δ sink is at a later time t_2. The interpolating fields $\chi^p(x)$ and $\chi^{\Delta^+}_\sigma(x)$ create an initial trial state with the proton and the Δ quantum numbers. We use smearing techniques in order to maximize the overlap to the initial trial states to the true hadronic states. The matrices Γ are projections for the Dirac indices [4]. Provided the Euclidean time separations t_1 and $t_2 - t_1$ are large enough, the time dependence and field renormalization constants cancel in the ratio

$$\begin{aligned} &R_\sigma(t_2,t_1;\mathbf{p}\,',\mathbf{p}\ ;\Gamma;\mu) = \\ &\frac{\langle G^{\Delta j^\mu N}_\sigma(t_2,t_1;\mathbf{p}\,',\mathbf{p};\Gamma)\rangle}{\langle G^{\Delta\Delta}_{ii}(t_2,\mathbf{p}\,';\Gamma_4)\rangle}\left[\frac{\langle G^{\Delta\Delta}_{ii}(t_2,\mathbf{p}\,';\Gamma_4)\rangle}{\langle G^{NN}(t_2,\mathbf{p};\Gamma_4)\rangle}\,\frac{\langle G^{NN}(t_2-t_1,\mathbf{p};\Gamma_4)\rangle\ \langle G^{\Delta\Delta}_{ii}(t_1,\mathbf{p}\,';\Gamma_4)\rangle}{\langle G^{\Delta\Delta}_{ii}(t_2-t_1,\mathbf{p}\,';\Gamma_4)\rangle\ \langle G^{NN}(t_1,\mathbf{p};\Gamma_4)\rangle}\right]^{1/2} \\ &\qquad \overset{t_2-t_1\gg 1, t_1\gg 1}{\Rightarrow} \Pi_\sigma(\mathbf{p}\,',\mathbf{p}\ ;\Gamma;\mu)\ . \end{aligned} \tag{6}$$

We always consider a frame where the Δ is at rest and therefore $\mathbf{q} = \mathbf{p}' - \mathbf{p} = -\mathbf{p}$. $Q^2 = -q^2$ is the Euclidean momentum transfer squared. Determining $\Pi_\sigma(\mathbf{q}\ ;\Gamma;\mu)$ for given values of σ and Γ by fitting to the plateau of $R_\sigma(t_2,t_1;\mathbf{p}\,',\mathbf{p}\ ;\Gamma;\mu)$ enables us to obtain the Sachs form factors. At the hadronic level, with the inclusion of complete sets of baryonic states and the use of Dirac and Rarita-Schwinger spinors the ratio of Eq. (6) leads to linear relations for the form factors. A convenient method for the evaluation of three-point functions is the *sequential inversion through the sink*. This requires fixing the state at t_2 have the quantum numbers of Δ with a fixed vector index σ. The projection

matrices Γ at the sink are also fixed. With one sequential inversion one can then evaluate the three-point function for any operator inserted at any intermediate time t_1. A novelty of our work is the construction of linear combinations of $\Pi_\sigma(\mathbf{q}\,;\Gamma;\mu)$, which project to either magnetic or quadrupole form factors and are optimized in the sense that the a maximal number of statistically independent measurements contribute to a given Q^2. This improves considerably the statistical accuracy that we obtained for the form factors. The optimized combination used for extracting $\mathcal{G}_{M1}$ is:

$$S_1(\mathbf{q};\mu) = \sum_{\sigma=1}^{3} \Pi_\sigma(\mathbf{q}\,;\Gamma_4;\mu) = iA\Big\{(p_2-p_3)\delta_{1,\mu} + (p_3-p_1)\delta_{2,\mu} + (p_1-p_2)\delta_{3,\mu}\Big\}\mathcal{G}_{M1}(Q^2) \quad .$$

The kinematical constant A and the combinations used for extracting $\mathcal{G}_{E2}$ and $\mathcal{G}_{C2}$ can be found in Ref. [12]. The full set of lattice measurements of these optimal matrix elements for all possible values of μ and $\mathbf{q}$ that give the same Q^2 are analyzed simultaneously through the solution of the overconstrained system of measured ratios extracting the three form factors.

In Fig. 1 we present the results for $\mathcal{G}_{M1}$ from all our ensembles. As can be seen there is agreement between the results obtained in the hybrid scheme where we use staggered sea quarks and domain wall valence quarks and those obtained with Wilson fermions. Performing a linear extrapolation in m_π^2 yields results at the physical point that are higher than experiment. We expect such a linear behavior to break down as the pion mass decreases for low Q^2 values. However we do not have a description from chiral theory on the dependence of these quantities on the pion mass. The R_{EM} and R_{SM} ratios

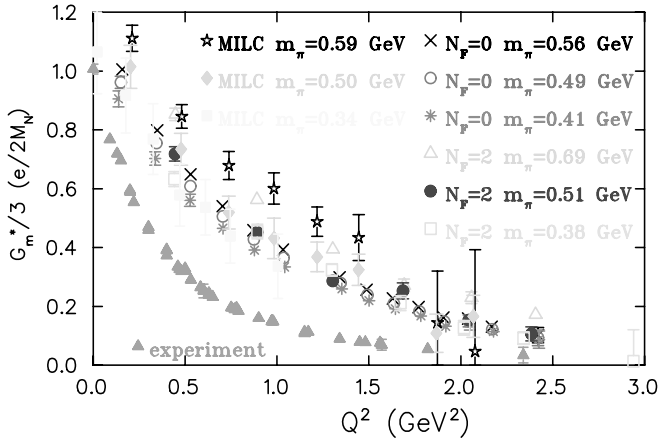

Figure 1. $G_m^*(Q^2) \equiv 1/\sqrt{1+Q^2/(m_N+m_\Delta)^2}\,\mathcal{G}_{M1}(Q^2)$ as function of Q^2. Experimental results from Ref. [13] are shown by the filled triangles.

are shown in Fig. 2. Results are shown for the Wilson ensembles only since the signal in the hybrid scheme is too noisy to allow a comparison. In the Wilson theory negative values are favored in agreement to experiment. Given that these form factors are suppressed by two orders of magnitude as compared to the dominant magnetic dipole form factor, being

able to confirm a negative non-zero value even in the quenched theory presents a major step forward. We have included results from several recent experiments as well as results from dynamical models. It is worth noting that a one-loop chiral effective theory with explicit N and Δ degrees of freedom [15] predicts the quark mass dependence of these ratios for small Q^2 and confirms that our lowest Q^2 data are in fact consistent with the experimental results at the physical point.

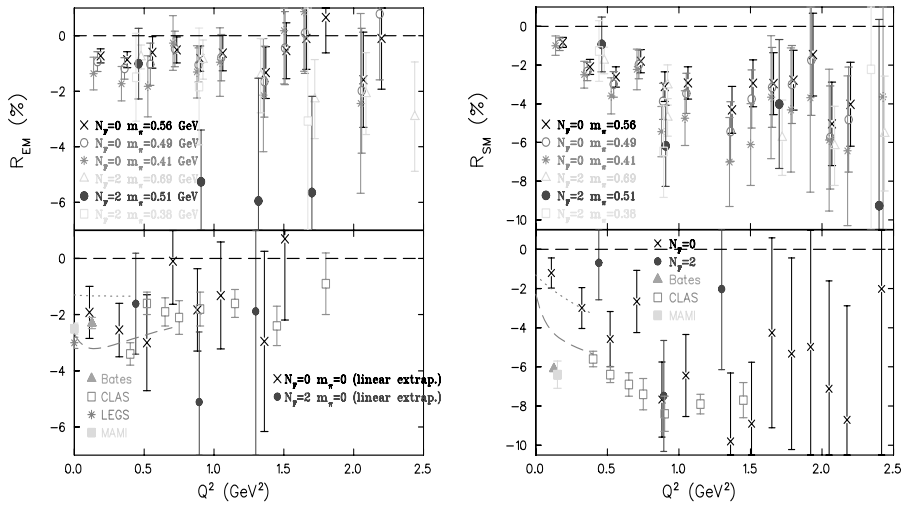

Figure 2. R_{EM} (left) and R_{SM} (right) as a function of Q^2. The lower graphs show linear extrapolations to the chiral limit for quenched (crosses) and unquenched (filled circles) Wilson fermions. We include recent experimental results from Refs. [6–9]. The dotted and dashed lines are the results from a dynamical model with bare and dressed vertices respectively [14].

3. NUCLEON ELECTROMAGNETIC FORM FACTORS

Recent polarization transfer experiments [16] have detected a q^2-dependence for the ratio of electric to magnetic form factor, $\mu_p G_E^p/G_M^p$, qualitatively different from that found using the standard Rosenbluth separation. Understanding the almost linear fall off of this ratio with $-q^2$ from QCD is one of hte main motivation of studying the nucleon form factors on the lattice.

The nucleon electromagnetic matrix element for real or virtual photons can be written in the form

$$\langle\, N(p',s')\,|j_\mu|\,N(p,s)\rangle = \left(\frac{M_N^2}{E_N(\mathbf{p}')\,E_N(\mathbf{p})}\right)^{1/2} \bar{u}(p',s')\left[\gamma_\mu F_1(q^2) + \frac{i\sigma_{\mu\nu}q^\nu}{2M_N}F_2(q^2)\right]u(p,s) \quad (7)$$

where we use the same notation as in the Section II. F_1, F_2 are the Dirac form factors with $F_1(0) = 1$ for the proton due to current conservation and $F_2(0)$ measures the anomalous

magnetic moment. They are connected to the electric, G_E, and magnetic, G_M, Sachs form factors by the relations

$$G_E(q^2) = F_1(q^2) + \frac{q^2}{(2M_N)^2} F_2(q^2) \quad , \quad G_M(q^2) = F_1(q^2) + F_2(q^2) \quad . \tag{8}$$

Constructing a ratio analogous to that given in Eq. (6) for the N to Δ transition we can extract the two form factors in the large Euclidean time limit. The optimal combinations of sequential nucleon sinks are easily constructed and provide independent determinations of G_M and G_E, each requiring one sequential inversion [5]. Unlike the $\gamma N \to \Delta$ transition, the $\gamma N \to N$ transition contains isoscalar photon contributions. This means that disconnected loop diagrams also contribute. These are generally difficult to evaluate accurately since the all-to-all quark propagator is required. In order to avoid disconnected diagrams, we calculate the isovector form factors. Assuming $SU(2)$ isospin symmetry, it follows that

$$\langle\, p\,|(-\bar{u}\gamma^\mu u - -\bar{d}\gamma^\mu d)|p\rangle - \langle\, n|(-\bar{u}\gamma^\mu u - -\bar{d}\gamma^\mu d)|n\rangle \qquad \langle\, p\,|(\bar{u}\gamma^\mu u - \bar{d}\gamma^\mu d)|p\rangle. \tag{ }$$

We therefore calculate directly the three-point function related to the right hand side of the above relation which provides the *isovector* nucleon form factors

$$G_E(q^2) = G_E^p(q^2) - G_E^n(q^2) \quad , \quad G_M(q^2) = G_M^p(q^2) - G_M^n(q^2). \tag{10}$$

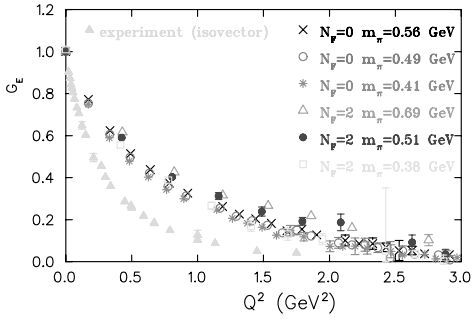

Figure 3. G_E as a function of Q^2 for Wilson fermions. Filled triangles show experimental results extracted using the analysis of Ref. [5].

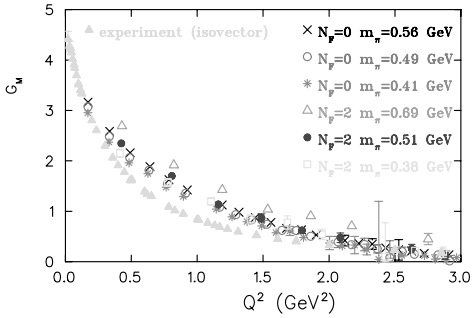

Figure 4. The isovector magnetic form factor, G_M, as a function of Q^2. The notation is the same as in Fig. 3.

Ensembles of quenched and two-flavor dynamical Wilson configurations are used to extract G_M and G_E for pion masses ranging from 690 down to 380 MeV. To convert the Q^2 into physical units we use the lattice spacing determined from the nucleon mass at the physical point. This gives $a^{-1} = 2.14$ GeV for the quenched theory and $a^{-1} = 2.56$ GeV for the unquenched theory. The results are G_E shown in Figs. 3, 4. In order to compare with experiment extrapolation to the chiral limit is needed. For these pion masses a linear

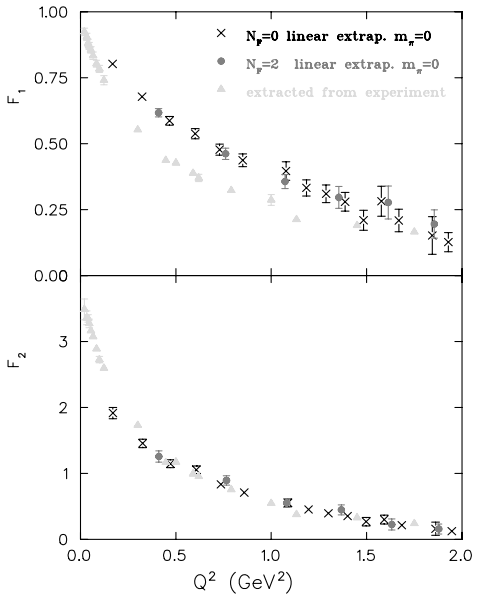

Figure 5. e rm ac rs F_1 (pper) an F_2 (l er) as a nc i n Q^2. r sses (. lle circles) s enc e (n enc e) res l s a e c iral limi . es l s e rac e r m e perimen are s n e lle riangles.

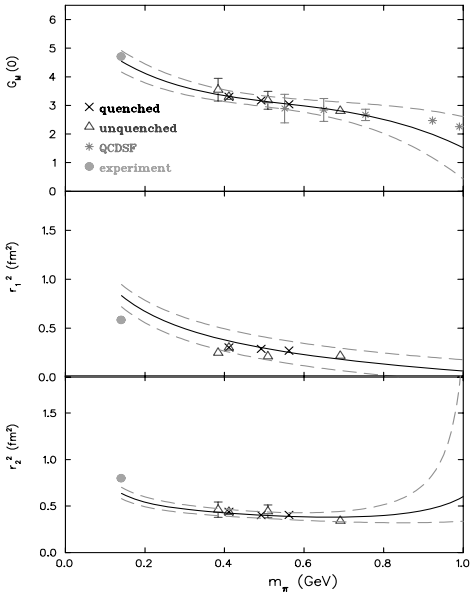

Figure 6. iral e rap la i n e magne ic m men an e r.m.s ra ii r_1 an r_2. e s li line is e es e e ec i e c iral e r res l s. e as e lines s e ma imal all e err r an sing e er- r rs n e e parame ers.

dependence on m_π^2 is consistent with the data. We therefore extrapolate linearly in m_π^2 to obtained results in the chiral limit. The Dirac form factors F_1 and F_2 are shown at the chiral limit in Fig. 5. F_2 is closer to experiment than F_1. In order to extract the magnetic moments we need to extrapolation to $Q^2 = 0$. Assuming a dipole Ansatz for both form factors with different dipole squared masses M_m and M_e,

$$G_M(Q^2) = \frac{G_M(0)}{\left(1 + \frac{Q^2}{M_m}\right)^2} \quad , \quad G_E(Q^2) = \frac{1}{\left(1 + \frac{Q^2}{M_e}\right)^2} \tag{11}$$

we obtain a good description of the data: The r.m.s. radius of the nucleon is determined from the slope of the form factor at $Q^2 = 0$. Therefore it can be computed directly from the dipole mass via

$$< r_i^2 >= -\frac{6}{F_i(Q^2)} \frac{dF_i(Q^2)}{dQ^2}|_{Q^2=0} = \frac{12}{M_i} \, , \quad i = 1, 2 \quad . \tag{12}$$

Pion cloud contributions are expected to become important as the pion mass decreases and therefore we expect deviations from the linear dependence on m_π^2. Recently, the quark mass dependence of the isovector magnetic moment and radii was determined within a

chiral effective theory with explicit nucleon and Δ degrees of freedom [17,18] at one-loop order. The expressions involve phenomenological parameters such as g_A, c_A, c_V, F_π and regularization counterterms. Following [18] we fit the expressions to the lattice data obtaining the maximal allowed error bands shown in Fig. 6.

4. SUMMARY

Fundamental questions connected to nucleon structure can be addressed from first principles using Lattice QCD. Optimized calculations of three-point functions with different formulations and systematics yield consistent results. We have confirmed for the first time in Lattice QCD, the existence of quadrupole strength in the N to Δ transition, in qualitative agreement with experiment. We have also presented a precise evaluation of the isovector nucleon form factors that show interesting behavior: the magnetic form factor is close to experiment whereas the electric is not. Whether such behavior is due to lattice artifacts or differences in the pion mass dependence of these form factors remains an open question. Such questions will be addressed as simulations at lighter quark masses and finer lattices become available.

Acknowledgments: A. T. acknowledges support from the program "Pythagoras" of the Greek Ministry of Education and from the University of Cyprus.

REFERENCES

1. K. Wilson, Phys. Rev. **D 10**, 245 (1974).
2. D. Kaplan, Phys. Lett. **B288**, 342 (1992); Y. Shamir, Nucl. Phys. **B406**, 90 (1993).
3. R. Narayanan and H. Neuberger, Phys. Lett. **B302**, 62 (1993); Phys. Rev. Lett. **71** 3251 (1993) ; P. Hasenfratz and F. Nidermayer, Nucl. Phys. **B414**, 785 (1994).
4. C. Alexandrou *et al.* Phys. Rev. Lett. **94**, 021601 (2005).
5. C. Alexandrou, G. Koutsou, J.W. Negele and A. Tsapalis, Phys. Rev. D **74**, 034508 (2006).
6. C. Mertz *et al.*, Phys. Rev. Lett.**86**, 2663 (2001).
7. K. Joo *et al.*, Phys. Rev. Lett. **88**, 122001 (2002).
8. G. Blanpied *et al.*, Phys. Rev. Lett. **79**, 4337 (1997).
9. R. Beck *et al.*, Phys. Rev. C **61**, 035204 (2000).
10. H. F. Jones and M.C. Scadron, Ann. Phys. (N.Y.) **81**, 1 (1973).
11. C. Alexandrou *et al.*, Phys. Rev. D **69**, 114506 (2004).
12. A. Tsapalis, Nucl. Phys. Proc. Suppl. 153, 320 (2006).
13. W. W. Ash *et al.*, Phys. Lett. **B24**, 165 (1967); D. Arndt and B. C. Tiburzi, Phys. Rev. D **69**, 014501 (2004); W. Bartel *et al.*, Phys. Lett. **B28**, 148 (1968); J.C. Alder *et al.*, Nucl. Phys. **B 46**, 573 (1972); K. Bätzner *et al.*, Phys. Lett. **B39**, 575 (1972); S. Stein *et al.*, Phys. Rrev. D **12**, 1884 (1975).
14. T. Sato and T.-S. H. Lee, Phys. Rev. C**63**, 055201 (2001).
15. V. Pascalutsa and M. Vanderhaeghen, Phys. Rev. Lett. **95**, 232001(2005)
16. M. Jones *et al.* Phys. Rev. Lett. **84**, 1398 (2000); O. Gayou *et al.*, Phys. Rev. C **64**, 038202 (2001); O. Gayou *et al.*, Phys. Rev. Lett. **88**, 092301 (2002).
17. T. R. Hemmert and W. Weise, Eur. Phys. J. A **15**,487 (2002).
18. M. Gockeler *et. al*, Phys. Rev. D **71**, 034508 (2005).